



HAL
open science

Microgrid sizing and energy management using Benders decomposition algorithm

Célia Masternak, Simon Meunier, Stéphane Brisset, Vincent Reinbold

► **To cite this version:**

Célia Masternak, Simon Meunier, Stéphane Brisset, Vincent Reinbold. Microgrid sizing and energy management using Benders decomposition algorithm. Sustainable Energy, Grids and Networks, 2024, 38, pp.101314. 10.1016/j.segan.2024.101314 . hal-04549235

HAL Id: hal-04549235

<https://hal.science/hal-04549235v1>

Submitted on 24 Feb 2025

HAL is a multi-disciplinary open access archive for the deposit and dissemination of scientific research documents, whether they are published or not. The documents may come from teaching and research institutions in France or abroad, or from public or private research centers.

L'archive ouverte pluridisciplinaire **HAL**, est destinée au dépôt et à la diffusion de documents scientifiques de niveau recherche, publiés ou non, émanant des établissements d'enseignement et de recherche français ou étrangers, des laboratoires publics ou privés.



Distributed under a Creative Commons Attribution - NonCommercial - NoDerivatives 4.0 International License

Microgrid sizing and energy management using Benders' decomposition algorithm

Célia Masternak^{1,2}, Simon Meunier^{1,2,*}, Stéphane Brisset³, Vincent Reinbold^{1,2}

¹Université Paris-Saclay, CentraleSupélec, CNRS, GeePs, 91192 Gif-sur-Yvette, France

²Sorbonne Université, CNRS, GeePs, 75252 Paris, France

³Centrale Lille, Arts et Metiers Institute of Technology, Université de Lille, Junia, ULR 2697-L2EP, 59000 Lille, France

*Corresponding author at: GeePs, 11 Rue Joliot Curie, 91192 Gif-sur-Yvette, France.

E-mail address: simon.meunier@centralesupelec.fr (S. Meunier).

Abstract:

Microgrids are of increasing interest because they can facilitate the integration of renewable energy sources. To make the most of microgrids, optimization problems are formulated and solved to determine their optimal planning (i.e. sizing and energy management). However, these problems are complex and time-consuming to solve. In this article, we focus on a temporal decomposition based on Benders' algorithm to reduce computing time while still obtaining the optimal solution. The temporal decomposition divides the initial problem into subproblems with a smaller time interval. The first originality of this work is the proposition of a methodology to apply this temporal decomposition to mixed-integer linear problems for the optimal planning of microgrids. The second originality is the investigation of the influence of the following relevant parameters on the computing time of the temporal decomposition based on Benders' algorithm: decomposition period, nature of the problem, overall time horizon and number of CPUs. In addition, contrary to previous literature, our proposed method exhibits computing time reductions. They are of up to 5.6 times for the considered case studies. Our results also highlight the existence of a decomposition period that maximizes the performances. Besides, we find that the temporal decomposition is particularly efficient for mixed-integer linear problems with large time horizons and when more than 16 CPUs can be used. The proposed generic methodology and our results can notably be useful to researchers and to microgrids project holders who aim at finding the optimal sizing and operation of their microgrid within reduced computing time.

Highlights:

- A mixed-integer linear problem (MILP) is solved to optimize microgrid planning.
- Benders' algorithm performs the temporal decomposition of the optimization problem.
- Method applied to a case study where computing times are reduced up to 5.6 times.
- There is a decomposition period that minimizes computing times.
- Distributing evenly subproblems across CPUs is key for achieving high performance.

Keywords:

Microgrids, Planning, Sizing and energy management, Decomposition, Benders' algorithm, Computing time

Nomenclature

Abbreviations

ADMM	Alternating direction method of multipliers
CPU	Central processing unit
LP	Linear problem
MILP	Mixed integer linear problem
MINLP	Mixed integer nonlinear problem
NLP	Nonlinear problem
PV	Photovoltaic
RES	Renewable energy sources

Indices

s	Index for temporal decomposition
t	Time

Sets

\mathcal{T}	Time horizon
---------------	--------------

Variables

C_{bat}	Battery capacity (Wh)
e	Energy stored in the battery (Wh)
P_c	Charging battery power (W)
P_d	Discharging battery power (W)
P_{in}	Input active power (W)
P_{out}	Output active power (W)
P_p	Peak power of the PV panels (W)
P_{PV}	Power produced by the PV panels (W)
u_{bat}	Battery binary variable
u_g	Grid binary variable

Benders' algorithm variables

α	Master problem additional variable
e_{fin}^s	Final energy in the battery for subproblem s
e_{ini}^s	Initial energy in the battery for subproblem s
λ_j^s	Dual variable

Parameters

b_{bat}	Battery replacement indicator
b_{PV}	PV panels replacement indicator
C_{bat}^{max}	Maximum battery capacity (Wh)
c_{in}	Cost of the electricity bought from the grid (€/Wh)
C_{inv}	Investment cost (€)
$c_{inv,bat}$	Investment cost for the battery (€/Wh)
$c_{inv,PV}$	Investment cost for the PV panels (€/W _p)
C_{maint}	Discounted maintenance cost (€)

$C_{maint,bat}$	Maintenance cost for the battery (€/Wh.year)
$C_{maint,PV}$	Maintenance cost for the PV panels (€/W _p .year)
C_{op}	Discounted operation cost (€)
c_{out}	Cost of the electricity sold to the grid (€/Wh)
$C_{PV,loss}$	Loss coefficient for the PV panels
C_{repl}	Discounted replacement cost (€)
δ	Discount rate
e_{max}	Maximum energy in the battery (Wh)
e_{min}	Minimum energy in the battery (Wh)
ε	Stopping criterion
G_0	Reference irradiance (W/m ²)
G_{PV}	Irradiance on the plane of the PV panels (W/m ²)
η_c	Battery charging efficiency
η_d	Battery discharging efficiency
L	Lifespan of the system (years)
LB	Lower bound
L_{bat}	Battery lifespan (years)
LCC	Life-cycle costs (€)
L_{PV}	PV panels lifespan (years)
OC	Operation costs over a given time horizon (€)
p_c^{fix}	Coefficient to compute the maximal charging power (y-intercept value) (W)
p_c^{max}	Battery maximum charging power (W)
p_c^{var}	Coefficient to compute the maximal charging power (slope) (W/Wh)
p_d^{fix}	Coefficient to compute the maximal discharging power (y-intercept value) (W)
p_d^{max}	Battery maximum discharging power (W)
p_d^{var}	Coefficient to compute the maximal discharging power (slope) (W/Wh)
p_{in}^{max}	Maximum electricity bought from the grid (W)
p_{out}^{max}	Maximum electricity sold to the grid (W)
P_l	Electricity load of the dwelling (W)
p_p^{max}	Maximum peak power of the PV panels (W _p)
SOC_{min}	Minimum state of charge of the battery
SOC_{max}	Maximum state of charge of the battery
T	End of the time horizon (days)
t_{comp}	Computing time for the compact resolution (s)
t_{decopt}	Computing time for the temporal decomposition (s)
UB	Upper bound
$Z_{optimality}^s$	Value of the objective function of the operation subproblem s (€)

1 Introduction

Over the last decades, there has been a large deployment of renewable energy sources (RES). RES are expected to represent 45% of the European energy mix by 2040 [1]. Due to their intermittency, integrating these sources is a challenge since the supply-demand balance needs to be fulfilled at all times, and grid reinforcements might be needed [2][3]. Since RES can be distributed, the energy can be produced near consumption, and with this distributed energy production, the concept of microgrids has arisen [4]. A

microgrid is a system that includes distributed energy sources [5] such as photovoltaic panels, possibly distributed storage such as inter-seasonal thermal storage or battery, an energy management system and loads (curtailable or fixed) [5]. Storage systems are an essential component of microgrids as they absorb power production variations of RES [6]. They are also useful to improve the energy utilization efficiency and maximize profits [7]. There is a growing interest in microgrids since they are a great asset to ease the integration of RES [8], while ensuring grid stability [9], increasing resilience to outages [10], and improving flexibility [11]. Microgrids are also increasingly found in remote areas or where power system resilience is a crucial concern [12]. Thus, microgrids are related to the United Nations sustainable development goals 7 (Affordable and clean energy) and 13 (Climate action) [13]. A microgrid can operate in islanded or grid-connected mode [14], and has different geographic scales: from a dwelling [15] to a whole neighbourhood [16].

To make the most of microgrids and ensure that the system is secure and reliable, it is crucial to determine microgrids' optimal sizing and energy management [17]. Optimal microgrid sizing consists in finding the optimal capacity of each system component (e.g. battery, photovoltaic panels) that ensures adequate supply at minimum costs [18] and/or environmental impact [19]. Optimal energy management (also called optimal operation) consists in dispatching the different sources of power to achieve these objectives. To this end, mathematical models are used to establish optimization problems that are solved by microgrid energy management systems [20]. Finding both the optimal sizing and operation is challenging since the sizing result is impacted by the operation strategy: depending on how components are used, capacities may vary greatly [18][21]. Optimization problems applied to microgrids contain many variables (for sizing and operation) of different kinds (e.g. real, integer), numerous constraints, and integrate several temporal scales: short term to deal with the operation dynamic and long term to consider sizing [18].

These complex optimization problems are time-consuming to solve, some of them cannot even be solved with traditional solvers [22]. A potential solution to reduce computing times is the use of decomposition methods [23]. The purpose of decomposition methods is to find the optimal solution by breaking the optimization problem into smaller subproblems, easier to solve [23]. Decomposition methods may reduce computing times since the subproblems can be solved in parallel [24] and are thus a promising field of research. This article focuses on a temporal decomposition based on Benders' decomposition. For the sake of clarity, we will use "Benders' algorithm" to refer to "Benders' decomposition", to avoid confusion with the term "temporal decomposition".

1.1 Literature review

Decomposition methods have been used in several studies to reduce the complexity and computing times of optimization problems applied to microgrids. For instance, the Dantzig-Wolfe decomposition was used [22]. This decomposition is an iterative process with one master problem and several subproblems. Each iteration adds a new variable to the master problem [25]. Another method that was used is the Alternating Direction Method of Multipliers [26], which divides an optimization problem into several subproblems (without a master problem). At each iteration, each subproblem sends its solution to the other subproblems so they converge to find a solution to the global problem [27]. However, Benders' algorithm, also called L-shaped method for stochastic problems [28][29], seems to have particularly caught the interest of scientists to solve a large variety of optimization problems [24], and has proven to perform better than the Alternating Direction Method of Multipliers [30]. We will therefore focus on the literature that uses Benders' algorithm to solve optimization problems applied to microgrids. Benders' algorithm was introduced by J.F Benders in 1962 to solve mixed-variables (integers and continuous) programming problems [31]. Then Geoffrion generalized it to nonlinear convex problems [32]. The main idea behind Benders' algorithm is to decompose the problem to be solved into two groups of simpler problems, namely the master problem and the subproblem (or several subproblems) [33]. The master problem is a relaxed version of the original problem, containing only a subset of the original variables and the associated constraints [34][32]. The subproblem is the original problem with the variables obtained from the master problem being fixed [34][32]. Currently, Benders' algorithm is available in common solvers such as CPLEX.

Benders' algorithm has been used to tackle four challenges concerning optimization problems applied to microgrids. The first challenge is finding both the optimal sizing and operation. To this end, Yang et al. [35] used Benders' algorithm to decouple investment and operation. Another challenge is the handling of binary variables. Nagarajan and Ayyanar [36] decomposed their optimization problem into a master problem with binary variables and a linear subproblem using Benders' algorithm.

The third challenge is the handling of uncertainties due to weather conditions and/or users' behaviour. Stochastic scenarios of RES production and electrical loads can be constructed to account for these uncertainties. Wei et al. [37] used Benders' algorithm to determine the optimal planning of a multi-energy microgrid considering long-term and short-term uncertainties. The master problem determines the investments variables, and a subproblem per scenario is solved to find the optimal scheduling. The authors found that the performance of their decomposition method is better than the one of the compact resolution (resolution without decomposition), especially when the number of scenarios is high. In a similar way, Khodaei [38] used Benders' algorithm to have

one subproblem per scenario. An interesting result he obtained, is that the computing time of Benders' algorithm increases linearly with the number of binary variables, whereas for the compact resolution, it increases exponentially. Abdulgalil et al. [39] also used Benders' algorithm to have one subproblem per stochastic scenario.

The last challenge is the long-term optimization, as highlighted by Pecena et al. [40] and Mulkhopadhyay et al. [41]. In this article, we aim at accounting for the evolution of the electricity demand and of the irradiance over the years. Nevertheless, solving the entire optimization problem in a compact way leads to unreasonable computing times and might even be unfeasible on regular computers [18]. To face this challenge, a potential solution is using the temporal decomposition, which aims at reducing the time horizon of an optimization problem by dividing it into several problems with a smaller time horizon.

Some applications of temporal decomposition based on Benders' algorithm were found in the literature. In particular, Hemmati et al. [42] and Montoya-Bueno et al. [43] used Benders' algorithm to divide their original optimization problem into one master problem (for the investment decision) and several independent subproblems (one for each reduced time interval, such as one day).

The temporal decomposition is more challenging to perform when there are intertemporal constraints, for instance, when a system is equipped with a battery. Indeed, it is not possible to easily decouple the constraints in order to have a single independent subproblem per time interval since the subproblems are linked by the state of the storage. To tackle this issue, Kim et al. [44] used the optimality condition decomposition to divide the subproblem that arose from Benders' algorithm into several subproblems (one per time step) that were solved in parallel. Moreover, they decomposed their original mixed-integer nonlinear problem into a mixed-integer linear problem (MILP) and several nonlinear problems (NLP). Xiong et al. [45] aimed at finding the optimal dispatch of integrated energy systems under uncertainty. To reduce computing times, they decomposed, using Benders' algorithm, their problem into one day-ahead optimization problem and several intra-day dispatch problems (one problem per time step). Finally, Brisset and Ogier [46] performed a temporal decomposition based on Benders' algorithm to find the optimal sizing and operation of a hybrid railway power substation over a year. They have one master problem and they divide the year into days so that one subproblem is solved per day. Nevertheless, their temporal decomposition reaches the optimal solution with a computing time five times higher compared to the compact resolution (resolution without decomposition).

1.2 Research gaps, contributions to the research field and article structure

Analysis of the above literature allows drawing attention to several aspects that are insufficiently addressed in articles that investigate the temporal decomposition using Benders' algorithm. To our best knowledge, only two articles [45][46] performed a temporal decomposition based on Benders' algorithm to solve an optimization problem with intertemporal constraints. However, Xiong et al. [45] did not size the elements of their microgrid, and the subproblems that arose from the decomposition were linear problems (LP). Additionally, their decomposition is not suitable for long-term optimization (≥ 1 year) since they had one subproblem per timestep. Moreover, the authors of [46] only focused on LP and the railway sector. Furthermore, our methodology allows computing time reductions. Contrary to references [45][46], our proposed methodology allows to decompose the original problem into a master problem and multiple MILP subproblems, and therefore to integrate binary variables into the decomposition. Moreover, articles [45] and [46] did not study the parameters that may influence the performance of the temporal decomposition in terms of computing times. As detailed in the following paragraphs, through our literature review, we have identified four parameters that can be of interest with regard to the temporal decomposition: the decomposition period [46], the nature of the optimization problem (MILP or LP) [38], the time horizon [37] and the number of central processing units (CPUs), when subproblems are solved in parallel [24].

Influence of the decomposition period. We explained in the literature review that the temporal decomposition divides an optimization problem with a given time horizon into subproblems with a smaller time horizon (the decomposition period being the length of this smaller time horizon). The decomposition period is thus directly linked to the number of subproblems. Rahmaniani et al. [24] highlighted that the number of subproblems should not be larger than the number of variables of the master problem. It means that there is a compromise to find between the number of subproblems and the complexity of the master problem. This has not been studied in the literature whereas it might have a significant impact on the performance of the temporal decomposition.

Influence of nature of the problem. As explained in Section 1.1, Khodaei [38] found that when the number of adjustable loads (i.e. loads that can be curtailed or deferred) increases, the decomposition, using Benders' algorithm, into scenarios is more efficient. Increasing the number of adjustable loads is equivalent to increasing the number of binary variables. Therefore, we intuit that the nature of the problem (MILP or LP) may impact the performance of the temporal decomposition based on Benders' algorithm, but such influence has not been studied in the literature.

Influence of the time horizon. We have seen in the literature review that a large number of scenarios improves the performance of Benders' algorithm, in terms of computing time, compared to the resolution without decomposition [43][37][38]. A large time

horizon is similar to a large number of scenarios since we can envision a large time horizon as several scenarios with a smaller time horizon. Therefore, we might expect that a large time horizon will lead to better performance of the temporal decomposition, but this was not investigated in previous literature.

Parallel computation and influence of the number of CPUs. Rahmaniani et al. [24] highlighted that one of the main advantages of temporal decomposition is that it is suitable for parallel computation, which could drastically reduce computing times. This parallel computation was only performed by Kim et al. [44], but their temporal decomposition was not based on Benders' algorithm. Moreover, the computing time of the parallel computation is directly linked to the number of CPUs since a higher number of CPUs leads to a higher number of subproblems that can be solved simultaneously. However, the influence of the number of CPUs on the performance of the temporal decomposition based on Benders' algorithm was not investigated.

In this article, we use the temporal decomposition based on Benders' algorithm to solve long-term optimization problems applied to microgrids. The subproblems that arise from the decomposition are solved in parallel. Additionally, we investigate the impact of the decomposition period, the nature of the problem, the time horizon and the number of CPUs on the performance of the temporal decomposition in terms of computing times. The remainder of this article includes a detailed description of the method in Section 2. This Section presents Benders' algorithm, the models, and the optimization problem. In Section 3, we apply the methodology to a case study and investigate the impact of the four parameters described above on computing time. In Section 4, we present the limitations and implications of our work as well as ideas for future work.

2 Method

In Section 2.1, we describe Benders' algorithm. In Section 2.2, we present the considered application of Benders' algorithm: an optimization problem for the sizing and operation of microgrids, on which we perform temporal decomposition.

2.1 Benders' algorithm

2.1.1 Initial problem

We consider two vectors of variables X and Y . The objective of the optimization is to minimize a function f that depends on X and Y [32]:

$$\min_{X,Y} f(X,Y) \quad (1)$$

$$s. t. g_1(Y) \leq 0 \quad (2)$$

$$g_2(X) \leq 0 \quad (3)$$

$$g_3(X,Y) \leq 0 \quad (4)$$

We express f as: $f(X,Y) = f_1(Y) + f_2(X) + f_3(X,Y)$, $\forall (X,Y)$, with f_1, f_2 and f_3 convex functions.

Benders' algorithm aims at finding an optimal solution by dividing the original problem into a master problem and a subproblem. The master problem is solved under Y : the set of complicating variables. Once the solution of the master problem is found, the subproblem is solved considering a fixed set of variables \bar{Y} . Y is called a set of "complicating variables" because the optimization problem is easier to solve when Y is fixed. Benders' algorithm is an iterative process, each iteration solves both the master problem (see Section 2.1.2) and the subproblem (see Sections 2.1.3 and 2.1.4). Each iteration adds a new constraint (referred as cut) to the master problem. The resolution of the master problem gives a lower bound (LB) to the optimal solution, whereas the resolution of the subproblem gives an upper bound (UB). The iterative process stops when a stopping criterion is reached. If f and g_1, g_2 and g_3 are convex, the generalized Benders' algorithm method ensures the convergence to the global optimal solution [32].

2.1.2 Master problem

The master problem is a relaxation of (1) where the set of variables X does not appear.

$$\min_{\alpha,Y} f_1(Y) + \alpha \quad (5)$$

$$s. t. \{feasibility + optimality cuts\}$$

$$g_1(Y) \leq 0 \quad (6)$$

where α is a variable that is an approximation of the contribution of X to the objective function. At the first step of the iterative process, $\{feasibility + optimality cuts\}$ is empty. The optimality and feasibility cuts are constraints added to the master problem. These constraints add new bounds to the variable α so that it reaches the optimal value of $f_2(X) + f_3(X,Y)$. They are constructed

after solving the optimality and feasibility subproblems detailed in Sections 2.1.3 and 2.1.4 respectively. Since the master problem is a relaxation of the global problem, solving the master problem provides a lower bound (LB) of the optimal value. We denote by \bar{Y} and $\bar{\alpha}$ the solutions of the master problem. After each iteration, LB is updated:

$$LB = f_1(\bar{Y}) + \bar{\alpha} \quad (7)$$

2.1.3 Optimality subproblem

The optimality subproblem aims at finding the optimal set of variables X , while fixing Y to its value found by the master problem. It has the following form [34]:

$$\min_X f_2(X) + f_3(X, Y) \quad (8)$$

$$s. t. g_2(X) \leq 0 \quad (9)$$

$$g_3(X, Y) \leq 0 \quad (10)$$

$$Y = \bar{Y} \quad (11)$$

with \bar{Y} the fixed value of Y determined by the master problem. Let us note $Z_{optimality}$ the value of the objective function of the optimality subproblem and \bar{X} the solution of the optimality subproblem. We have:

$$Z_{optimality} = f_2(\bar{X}) + f_3(\bar{X}, \bar{Y}) \quad (12)$$

The following optimality cut is added to the master problem [32][25]:

$$\alpha \geq Z_{optimality} + \lambda' \cdot (Y - \bar{Y}) \quad (13)$$

where λ is a vector of dual variables associated with constraint (11) and λ' its transpose. Dual variables are also called “shadow price” or “marginalized cost”. They represent the utility gained (or lost) on the objective function if the constraint is relaxed by one unit. These variables are also used in nonlinear programming to compute the Karush-Kuhn-Tucker conditions.

Solving the optimality subproblem gives a feasible solution of the global problem. Therefore, it provides an upper bound (UB) for the optimal solution. After each iteration and if the subproblem is feasible, the upper-bound is updated:

$$UB = Z_{optimality} + f_1(\bar{Y}) \quad (14)$$

2.1.4 Feasibility subproblem

If the optimality subproblem is infeasible, the following feasibility subproblem is solved [32]:

$$\min_{\beta_1, \beta_2} \beta_1 + \beta_2 \quad (15)$$

$$s. t. g_2(X) \leq \beta_1 \quad (16)$$

$$g_3(X, Y) \leq \beta_2 \quad (17)$$

$$Y = \bar{Y} \quad (18)$$

where β_1 and β_2 are positive extra variables added to relax constraints (9) and (10). Let us note $Z_{feasibility}$ the value of the objective function of the feasibility subproblem. The following feasibility cut is added to the master problem [32]:

$$Z_{feasibility} + \mu' \cdot (Y - \bar{Y}) \leq 0 \quad (19)$$

with μ a vector of dual variables associated with constraint (18) and μ' its transpose. Note that, at every iteration, the size of the master problem increases since a new constraint is added. The iterative process described above continues until UB and LB converge within a predefined tolerance ε . The algorithm stops when we have $\frac{UB-LB}{LB} \leq \varepsilon$. The iterative process is summarized in Figure 1.

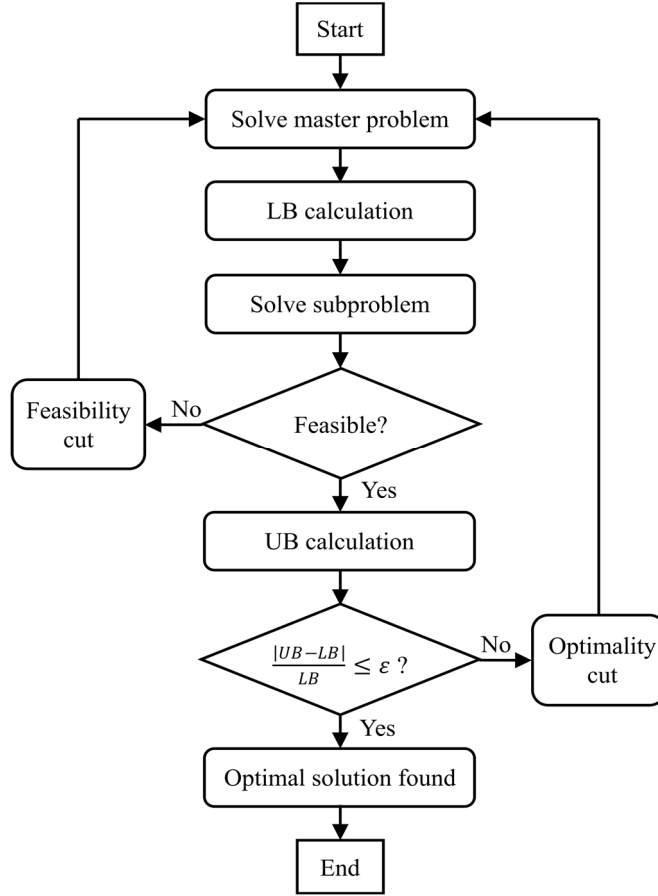


Figure 1: Flowchart for Benders' algorithm

2.2 Application of Benders' algorithm to microgrids optimization

In Section 2.2.1, we introduce the system considered, and in Section 2.2.2, the models used to formulate the optimization problem that is presented in Section 2.2.3. Finally, in Section 2.2.4, we formulate the temporal decomposition based on Benders' algorithm applied to our optimization problem.

2.2.1 System

In this article, we consider a dwelling as microgrid. It has its own electricity demand (appliances, lighting, heating, etc.), possesses a battery bank and photovoltaic (PV) panels and an energy management system. It exchanges power with the low-voltage distribution grid by buying or selling electricity.

2.2.2 Model

Battery bank. We consider the following bilinear model for the battery bank [47]:

$$\frac{de(t)}{dt} = P_c(t) \cdot \eta_c - \frac{P_d(t)}{\eta_d} \quad (20)$$

where η_c and η_d are the charging and discharging efficiencies respectively, $P_c(t)$ and $P_d(t)$ are the charging and discharging powers respectively, and $e(t)$ the energy stored in the battery at time t .

Photovoltaic panels. We consider that the maximum power point tracking of the PV panels is correctly performed and we compute the power produced by the PV panels $P_{PV}(t)$ using equation (21). This first-order equation introduces a fixed coefficient $c_{PV,loss}$ for all the PV system losses (e.g. temperature, soiling, wiring), which is considered sufficient for the purpose of this article. Note that there are more detailed models for computing the power produced by PV panels as the ones presented in [48].

$$P_{PV}(t) = \frac{G_{PV}(t)}{G_0} \cdot P_p \cdot (1 - c_{PV,loss}) \quad (21)$$

In Equation (21), $G_{PV}(t)$ is the irradiance on the plane of the PV panels, G_0 is the reference irradiance (1000 W/m²) and P_p is the peak power of the PV panels in standard test condition.

Grid exchanges. The instantaneous cost related to the grid exchange $c_{grid}(t)$, is given by [47]:

$$c_{grid}(t) = P_{in}(t) \cdot c_{in}(t) - P_{out}(t) \cdot c_{out}(t) \quad (22)$$

with $P_{in}(t)$ and $P_{out}(t)$ the power that the microgrid buys or sells from the grid respectively, and $c_{in}(t), c_{out}(t) \geq 0$ are the instantaneous prices for buying and selling electricity respectively.

2.2.3 Optimization problem

In this Section, we present the objective, constraints and degrees of freedom of the optimization problem.

Objective.

In this work, we aim at minimizing the life-cycle cost LCC [3][49]:

$$\min\{LCC\} = \min \{C_{inv} + C_{maint} + C_{repl} + C_{op}\} \quad (23)$$

where C_{inv} is the investment cost, C_{maint} the discounted maintenance cost, C_{repl} the discounted replacement cost and C_{op} the discounted operation cost.

The investment cost C_{inv} is given by:

$$C_{inv} = c_{inv,bat} \cdot C_{bat} + c_{inv,pv} \cdot P_p \quad (24)$$

where $c_{inv,bat}$ and $c_{inv,pv}$ are the unit investment costs for the battery bank and photovoltaic panels respectively, C_{bat} the battery capacity and P_p the peak power of the photovoltaic panels.

The discounted maintenance cost C_{maint} is given by [49]:

$$C_{maint} = \sum_{y=1}^L \frac{c_{maint,bat} \cdot C_{bat} + c_{maint,pv} \cdot P_p}{(1 + \delta)^y} \quad (25)$$

with δ the discount rate, L the considered lifetime of the system and $c_{maint,bat}$ and $c_{maint,pv}$ are the yearly unit maintenance costs for the battery bank and photovoltaic panels respectively.

The discounted replacement cost C_{repl} is given by [49]:

$$C_{repl} = \sum_{y=1}^L \frac{b_{bat}(y) \cdot c_{inv,bat} \cdot C_{bat} + b_{pv}(y) \cdot c_{inv,pv} \cdot P_p}{(1 + \delta)^y} \quad (26)$$

where $b_{bat}(y)$ and $b_{pv}(y)$ are indicators to assess whether the component (battery or PV) should be replaced at a given year y , depending on its lifetime. They are given by:

$$b_{bat}(y) = \begin{cases} 1 & \text{if } y = K \cdot L_{bat} \\ 0 & \text{otherwise} \end{cases} \quad (27)$$

$$b_{pv}(y) = \begin{cases} 1 & \text{if } y = M \cdot L_{pv} \\ 0 & \text{otherwise} \end{cases} \quad (28)$$

where K and M are integers and L_{bat} and L_{pv} are the lifetime of the battery and the PV panels respectively.

We compute the operation cost averaged over a year $OC(\mathcal{T})$ as follows [47]:

$$OC(\mathcal{T}) = \frac{365}{T} \cdot \sum_{t \in \mathcal{T}} (P_{in}(t) \cdot c_{in}(t) - P_{out}(t) \cdot c_{out}(t)) \delta_t \quad (29)$$

where T is the end of the time horizon \mathcal{T} ($\mathcal{T} = [0, T]$) and the coefficient $\frac{365}{T}$ is used to average the costs over a year. This cost $OC(\mathcal{T})$ is related to buying and selling electricity to the low-voltage grid. Then, the discounted operation cost C_{op} is given by:

$$C_{op} = \sum_{y=1}^L \frac{OC(\mathcal{T})}{(1 + \delta)^y} \quad (30)$$

Investment constraints.

We first introduce the investment constraints related to the capacity of the components. Regarding the battery, we limit its capacity c_{bat} as well as the energy stored in the battery $e(t)$:

$$C_{bat} \leq C_{bat}^{max} \quad (31)$$

$$e_{min} = SOC_{min} \cdot C_{bat} \leq e(t) \leq e_{max} = SOC_{max} \cdot C_{bat} \quad (32)$$

where SOC_{min} and SOC_{max} are the minimum and maximum state of charge of the battery and e_{min} and e_{max} the minimal and maximal energy stored in the battery. Equation (32) states that we cannot fully charge or discharge the battery. The maximum charging P_c^{max} and discharging P_d^{max} powers of the battery are expressed as a linear function of the installed capacity C_{bat} [22]:

$$P_c^{max} = P_c^{fix} + C_{bat} \cdot P_c^{var} \quad (33)$$

$$P_d^{max} = P_d^{fix} + C_{bat} \cdot P_d^{var} \quad (34)$$

with P_c^{fix} , P_c^{var} , P_d^{fix} and P_d^{var} coefficients to compute the maximum charging and discharging power using a linear form.

When it comes to the PV panels, we limit the peak power of the PV array by a maximum peak power P_p^{max} :

$$P_p \leq P_p^{max} \quad (35)$$

Operation constraints.

When charging and discharging efficiencies are considered (i.e. $\eta_c \neq 1$ and/or $\eta_d \neq 1$), it is necessary to introduce a binary variable $u_{bat}(t)$ to make sure that the battery is not charging and discharging at the same time [47]:

$$P_c(t) - u_{bat}(t) \cdot P_c^{max} \leq 0 \quad (36)$$

$$P_d(t) - (1 - u_{bat}(t)) \cdot P_d^{max} \leq 0 \quad (37)$$

where P_c^{max} and P_d^{max} are the maximum charging and discharging powers respectively.

The second operation constraint concerns the demand/supply balance. Indeed, the power balance of the dwelling (left side of Equation (38)) must be equal to the power that the dwelling buys or sells to the main grid (right side of Equation (38)):

$$P_l(t) + P_c(t) - P_d(t) - P_{pv}(t) = P_{in}(t) - P_{out}(t) \quad (38)$$

with $P_l(t)$ the electricity load of the dwelling.

The third operation constraint is related to the electricity exchanged with the low-voltage grid. To prevent the system from buying and selling electricity at the same time, we introduce $u_g(t) \in \{0,1\}$ such that:

$$P_{in}(t) - u_g(t) \cdot P_{in}^{max} \leq 0 \quad (39)$$

$$P_{out}(t) - (1 - u_g(t)) \cdot P_{out}^{max} \leq 0 \quad (40)$$

There are 2 constraints regarding the sizing degrees of freedom. Moreover, per time step, there are 4 constraints related to the battery, 1 constraint related to the power balance and 2 constraints related to the grid. If we consider a time horizon of 20 years with a time step of 15 minutes, there are $(4 + 1 + 2) \times 96 \times 365 \times 20 + 2 = 4,905,602$ constraints.

Degrees of freedom (decision variables).

The degrees of freedom (also called ‘‘decision variables’’) of the optimization problem are related to the sizing of the system with the battery capacity $C_{bat} \in [0, C_{bat}^{max}]$ and the peak power of the PV panels $P_p \in [0, P_p^{max}]$, and to its operation with the battery charging and discharging powers ($P_c(t) \in [0, P_c^{max}]$ and $P_d(t) \in [0, P_d^{max}]$). The use of operation related degrees of freedom can significantly increase the total number of degrees of freedom because, for each set of optimization degree of freedom (e.g. $P_c(t)$), there is one optimization degree of freedom per time step. For instance, if we consider a time horizon of 20 years with a time step of 15 minutes, this leads to 1,401,600 operation degrees of freedom ($2 \times 96 \times 365 \times 20 = 1,401,600$).

2.2.4 Temporal decomposition

Overall idea

In Section 1, we explained that the goal of the temporal decomposition is to reduce the time horizon of an optimization problem by dividing it into several problems with a smaller time horizon. For instance, if we consider a time horizon \mathcal{T} of one year, we can divide the original problem into $S (=52)$ weeks, which leads to S subproblems that are solved independently. In this case, the decomposition period, which corresponds to the length of each reduced time interval, is equal to one week. For the considered

system, the link between two reduced time intervals is the energy stored in the battery: the energy stored at the end of a time interval must be equal to the energy stored at the beginning of the following time interval.

Formulation

We use Benders' algorithm introduced in Section 2.1 to give a mathematical formulation for the temporal decomposition applied to the optimization problem described in Section 2.2.3.

It is possible to divide the global time horizon \mathcal{T} into S smaller time intervals:

$$\mathcal{T} = \mathcal{T}_1 \cup \dots \cup \mathcal{T}_S \quad (41)$$

This means that, using the temporal decomposition, we break the optimization problem into S subproblems, and s is the index referring to a specific subproblem.

The goal of the master problem is to make sizing decisions but also to determine intermediate states of the battery (at the end and at the beginning of each reduced time horizon). Therefore, the master problem is:

$$\min\{(C_{inv} + C_{maint} + C_{repl}) + \sum_s \alpha(s)\} \quad (42)$$

$$s.t. e_{min} \leq e_{ini}^s \leq e_{max}, \forall s \in \{1, \dots, S-1\} \quad (43)$$

$$e_{min} \leq e_{fin}^s \leq e_{max}, \forall s \in \{1, \dots, S-1\} \quad (44)$$

$$e_{fin}^s = e_{ini}^{s+1}, \forall s \in \{1, \dots, S-1\} \quad (45)$$

$$e_{ini}^0 = e_{min} \quad (46)$$

$$e_{fin}^S = e_{min} \quad (47)$$

{optimality cuts}

where e_{ini}^s and e_{fin}^s are the initial and final energy stored in the battery for the reduced time interval \mathcal{T}_s . The intermediate states link the subproblems, as indicated by Equation (45). Equations (46) and (47) specify that at the beginning and at the end of the time horizon, the state of charge of the battery is minimal. The master problem is also subject to the investment constraints (31) and (35) defined in Section 2.2.3. It should be noted that at the first iteration, {optimality cuts} is empty and therefore, the sizing variables are equal to their lower bound.

Each subproblem aims at finding the optimal operation during the reduced time interval \mathcal{T}_s . The subproblem s is:

$$\min \sum_{t \in \mathcal{T}_s} (c_{in}(t) \cdot P_{in}(t) - c_{out}(t) \cdot P_{out}(t)) \cdot \delta_t \quad (48)$$

$$s.t. e_{ini}^s = \overline{e_{ini}^s} \quad (49)$$

$$e_{fin}^s = \overline{e_{fin}^s} \quad (50)$$

$$C_{bat} = \overline{C_{bat}} \quad (51)$$

$$P_p = \overline{P_p} \quad (52)$$

where $\overline{e_{ini}^s}$, $\overline{e_{fin}^s}$, $\overline{C_{bat}}$ and $\overline{P_p}$ are fixed and determined by the master problem. The operation subproblems are also subject to the operation constraints (36)-(40) defined in Section 2.2.3.

The following optimality cuts are added to the master problem for the next iteration:

$$\alpha(s) \geq Z_{optimality}^s + \lambda_1 \cdot (e_{ini}^s - \overline{e_{ini}^s}) + \lambda_2 \cdot (e_{fin}^s - \overline{e_{fin}^s}) + \lambda_3 \cdot (C_{bat} - \overline{C_{bat}}) + \lambda_4 \cdot (P_p - \overline{P_p}) \quad (53)$$

with $\lambda_1, \lambda_2, \lambda_3$ and λ_4 the dual variables associated to the constraints (49), (50), (51) and (52) and $Z_{optimality}^s$ the value of the objective function of the operation subproblem s .

We have seen in Section 2.1 that the iterative process of Benders' algorithm includes the resolution of a feasibility subproblem. In this case, the energy stored in the battery determined by the master problem is always achievable by the operation subproblem since the dwelling can buy or sell electricity to the low-voltage grid, provided that the energy exchanged between the dwelling and the grid does not reach the grid capacity constraints. Therefore, in this case, we only solve optimality subproblems. Otherwise, if the

operation subproblem is infeasible due to the grid constraints, extra positive variables can be added to the constraint on the intermediate battery energy and the associated feasibility subproblem can be defined.

The subproblems are MILP. It is not possible to retrieve dual variables of those mixed-integer subproblems with common solvers. It is therefore not possible to formulate the optimality cuts (53). To tackle this issue, we solve the operation subproblem a first time, store the binary variables and solve the operation subproblem a second time with fixed binary variables [43]. This operation provides the weak dual variables associated with constraints (49)-(52) [50]. The flowchart for the temporal decomposition is presented in Figure 2.

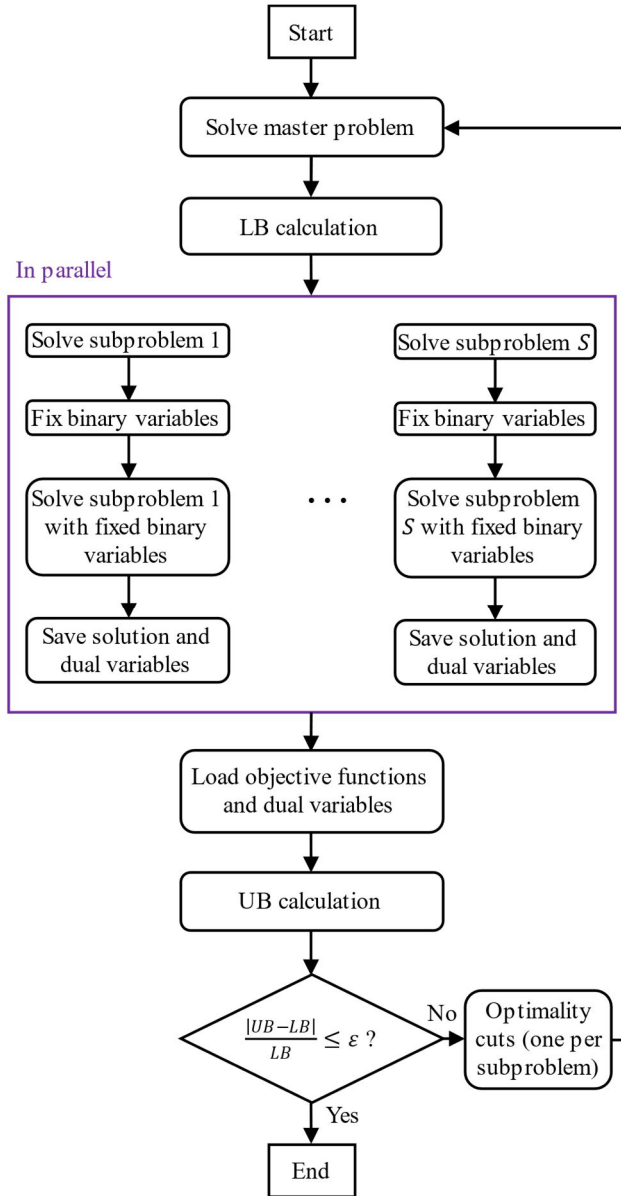


Figure 2: Flowchart for the temporal decomposition

If we consider a time horizon of 1 year and a temporal decomposition in weeks (i.e. we have 52 subproblems), the master problem has 2 sizing degrees of freedom (battery capacity and solar panel peak power) and 51 degrees of freedom for the intermediate states of the battery. Therefore, the master problem has $2+51 = 53$ degrees of freedom. Moreover, assuming that we have a time step of 15 minutes, each subproblem has $7 \times 96 \times 2 = 1,344$ degrees of freedom (because there are 2 operation degrees of freedom per time step).

2.2.5 Implementation

The optimization problems are implemented with Pyomo, a Python-based package used to formulate optimization problems [51]. Pyomo is an algebraic modelling language. Therefore, the master problems and subproblems described in Section 2.2.4 are

implemented using the mathematical equations involving parameters, variables and their derivative. When the derivative of a variable is needed, we use *DerivativeVar* from the *pyomo.DAE* modelling extension which allows to use differential algebraic equations in a Pyomo model.

The models of the components are implemented, within a *pyomo.Block* class, using the equations presented in Sections 2.2.2 and 2.2.3. The equations are implemented in their continuous form using the *pyomo.Constraint*, *pyomo.Expression* or *pyomo.Integral*, when necessary. The components models are gathered in the library LMS2 [52]. The idea behind the LMS2 library [52] is to structure general models that can be put together to easily create optimization problems of complex systems. The subproblems are instantiated by a *pyomo.Block* called “microgrid block”. This block holds the blocks of each component and links them through *pyomo.Constraint* (such as the power balance) and an objective function defined by the user. Once all the subproblems are instantiated, the discretization is automatically made using a Pyomo transformation. In our case, we use a simple finite difference method. Once the problem is constructed, we load the data. The iterative process of the temporal decomposition is illustrated in Figure 2 and implemented using a while loop.

The problems are solved with Gurobi. To solve linear models, Gurobi uses the simplex algorithm and for MILP, it uses a branch-and-cut algorithm. Moreover, Pyomo dual variables values are easily accessible: one just needs to signal that duals are desired before solving the optimization problem.

The calculations are done in a high-performance computing center (the “Moulon Mésocentre” [53] in our case). When the main script is launched on a node of the computing center, the user specifies the number of CPUs to use (which is, in the “Moulon Mésocentre”, equivalent to the number of threads). A set of tasks specific to one subproblem is performed on one CPU. These sets of tasks are performed in parallel using the Python package *mpi4py*, as recommended when solving in parallel problems modelled with Pyomo. In our case, we have access to a node with a maximum of 40 CPUs of 2.1 GHz each.

3 Case study

In this Section, we investigate the parameters that influence the performance of the temporal decomposition on a case study. The study parameters are presented in Section 3.1 and the results in Section 3.2.

3.1 Study parameters

We consider a dwelling located in Hamelin, Germany (Latitude: 52.1°, Longitude: 9.37°). The value considered for the study parameters are provided in Table 1. For illustration purposes, in Figure 3, we plot the irradiance and electricity demand for the three first days of the input data.

Table 1: Parameters for the case study

Parameter	Symbol	Value
Battery bank		
Maximum capacity	C_{bat}^{max}	48,000 Wh [54]
Investment cost	$c_{inv,bat}$	0.47 €/Wh [18][54]
Maintenance cost	$c_{maint,bat}$	10^{-3} €/Wh.year [18][54]
Minimum state of charge	SOC_{min}	0.2 [55]
Maximum state of charge	SOC_{max}	0.9 [18]
Fixed charging power	p_c^{fix}	2190 W [22]
Variable charging power	p_c^{var}	0.443 W/Wh [22]
Fixed discharging power	p_d^{fix}	2433 W [22]
Variable discharging power	p_d^{var}	0.148 W/Wh [22]
Charging efficiency	η_c	0.9776 [22]
Discharging efficiency	η_d	0.9776 [22]
Lifetime	L_{bat}	10 years [56][57]
Photovoltaic (PV) panels		
Maximum peak power of the PV panels	p_p^{max}	10000 W _p [58]
Investment cost	$c_{inv,pv}$	1.5 €/W _p [59]
Maintenance cost	$c_{maint,pv}$	6×10^{-3} €/W _p .year [18]
Loss coefficient	$c_{pv,loss}$	0.19 [60]
Lifetime	L_{pv}	20 years [61][62] *
Grid		
Cost of the electricity bought from the grid	c_{in}	0.56 €/kWh [63]
Cost of the electricity sold to the grid	c_{out}	0.082 €/kWh [58]
General		
Considered lifetime of the system	L	20 years [18]
Discount rate	δ	0.05 [2]
Optimization		
Time step	δ_t	15 min
Stopping criterion for Benders' algorithm	ϵ	10^{-3} [44]
Input data		
Irradiance	$G_{pv}(t)$	Time series from [64] - Mean irradiance: 135 W/m ² - Maximal irradiance: 1072 W/m ²
Electricity demand	$P_i(t)$	Time series from [65] - Mean demand: 1354 W - Maximal demand: 6071 W

Note: * There are more accurate PV panels models that consider the aging of panels along their lifetime depending on several factors (e.g. technology, location [66]).

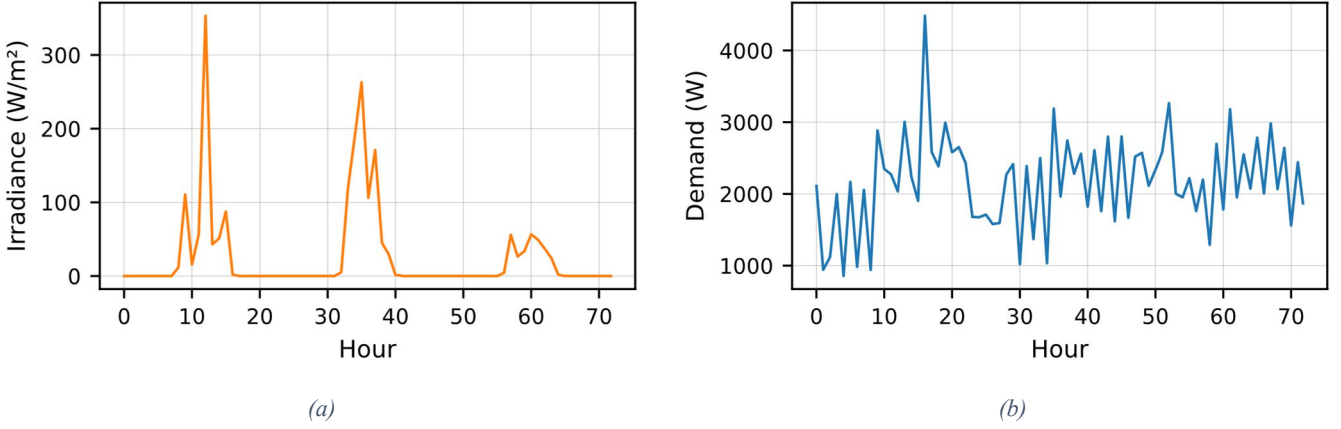


Figure 3: Temporal evolution of (a) the irradiance and (b) the electricity demand for the three first days of the input data

3.2 Results

In this Section, we study the influence of the following parameters on the performance of the temporal decomposition in terms of computing time: the decomposition period (Section 3.2.1), the nature of the problem (MILP or LP) (Section 3.2.2), the time horizon (Section 3.2.3), and the number of CPUs (Section 3.2.4).

3.2.1 Influence of the decomposition period

In this Section, we solve the optimization problem introduced in Section 2.2.3, over one year and study the influence of the decomposition period on the computing times. We remind that the “compact resolution” refers to the resolution of the optimization problem without decomposition, and that the decomposition period corresponds to the length of a reduced time interval. In Table 2, we summarize the optimization results for the compact resolution and the temporal decomposition using 9 days as decomposition period, which corresponds to one subproblem per CPU (i.e. 40 subproblems).

Table 2: Results comparison with the compact resolution and the temporal decomposition

		Compact resolution	Temporal decomposition
Time horizon: 1 year	Life-cycle cost LCC	63,890 €	63,911 €
	Battery capacity C_{bat}	5,9 kWh	6,6 kWh
Number of subproblems per CPU: 1	PV peak power P_p	10 kW	10 kW
	Computing time	3 min 36 s	4 min 4 s

First, we notice that the results in terms of life-cycle costs are extremely close (error of 0.03%) between the compact resolution and the temporal resolution. Regarding the variables values, there is a difference of 12% for the battery capacity and none for the peak power of the PV panels. In this case, the temporal decomposition converges 28 seconds slower than the compact resolution.

In Figure 4, we plot the computing times ratio t_{decopt}/t_{comp} as a function of the ratio of the time horizon over the decomposition period: T/T_s . The black horizontal line corresponds to $t_{decopt}/t_{comp} = 1$. Below this line the performance of the decomposition is better than the compact resolution and above it is worse. Note that the ratio T/T_s is also equal to the number of subproblems. In Figure 4, we observe that the number of subproblems has a strong influence on the performance of the temporal decomposition: when the number of subproblems is equal to 20, the computing time is lower with the temporal decomposition. There is a ratio ($T/T_s = 20$) that maximizes the performance of the temporal decomposition: the temporal decomposition is 1.2 times faster than the compact resolution for this ratio. Above 20 subproblems, the temporal decomposition becomes inefficient (up to 17 times slower than the compact resolution). Indeed, there are too many subproblems (compared to the number of variables of the initial problem) to see the benefits of the decomposition.

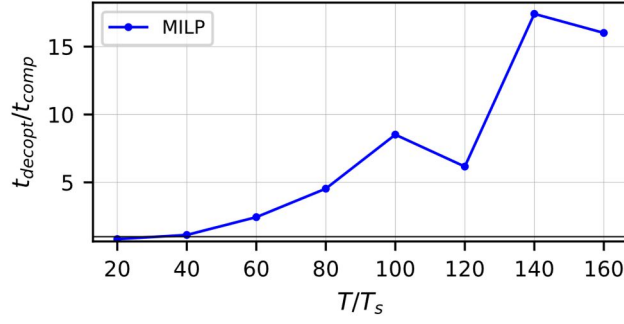


Figure 4: Influence of the decomposition period on the computing time
 Note: the horizontal line corresponds to $t_{decept}/t_{comp} = 1$

3.2.2 Influence of the nature of the problem

The optimization problem solved in Section 3.2.1 is a MILP. We found that the temporal decomposition leads to lower computing times, when the number of subproblems is equal to 20. In this Section, we investigate if the temporal decomposition is still efficient when the problem is linear. To this end, we transform the problem described above into a LP. To get rid of binary variables, we make the following changes:

- Charging and discharging efficiencies are considered equal to 1.
- Impossibility to export electricity: the surplus of production is lost.

Similar to the results presented in Section 3.2.1, we solve the optimization problem for several decomposition periods. In Figure 5, we plot the variation of the computing times ratio for the LP (red line) and MILP (blue line) as a function of the ratio T/T_s . Both optimizations were performed for a time horizon of 1 year. First, we observe that both curves have a similar shape and that the ratio that maximizes the performance of the temporal decomposition is identical for both cases ($T/T_s = 20$). An important result is that for the LP, the temporal decomposition always reaches a solution with higher computing times than the compact resolution. The temporal decomposition has an interest only in the case of MILP for the considered case study. Indeed, the linear problem is relatively easy to solve and the additional operations for data saving and loading introduced by the temporal decomposition do not allow to reduce computing times.

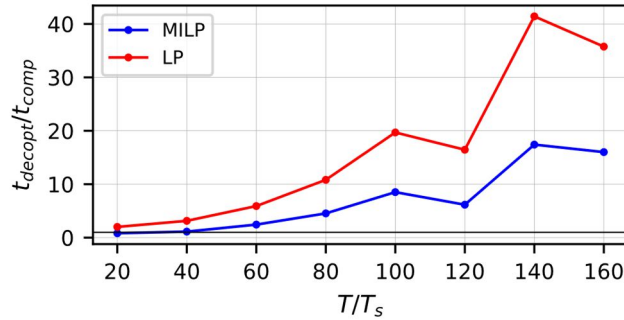


Figure 5: Influence of the nature of the problem on the computing time
 Note: the horizontal line corresponds to $t_{decept}/t_{comp} = 1$

3.2.3 Influence of the time horizon

In this section, we investigate the influence of the time horizon on the performance of the temporal decomposition for large time horizons: 1 year, 10 years, and 20 years. The largest time horizon is 20 years because it corresponds to the considered lifespan of the overall system.

In Table 3, we summarize the results of the optimization for the ratios that give the best performance for each time horizon: 20, 40 and 80 for 1 year, 10 years and 20 years respectively. The absolute difference in computing time between both resolution methods is the highest for the largest time horizon (20 years): ~ 96 minutes. The performance of the temporal decomposition improves with the increase of the time horizon.

Table 3: Results comparison between the compact resolution and the temporal decomposition (using the optimal decomposition period) for several time horizons

		Compact resolution	Temporal decomposition	Ratio of computing times
Time horizon: 1 year Number of subproblems per CPU: 0.5	LCC	63,890 €	63,895 €	
	Computing time	3 min 37 s	2 min 59 s	0.82
Time horizon: 10 years Number of subproblems per CPU: 1	LCC	65,244 €	65,259 €	
	Computing time	40 min 2 s	11 min 27 s	0.29
Time horizon: 20 years Number of subproblems per CPU: 2	LCC	64,793 €	64,800 €	
	Computing time	117 min 22 s	21 min 16 s	0.18

In Figure 6, we plot the variation of the computing times ratio as a function of the number of subproblems (T/T_s) for several time horizons (1, 10 and 20 years). For each time horizon, there is a decomposition period (i.e. ratio T/T_s) that maximizes the performance of the temporal decomposition. We notice that the larger the time horizon, the larger the ratio T/T_s that gives the best performance. The best decomposition period is a compromise between the number of subproblems and their complexity: if T/T_s is too low, the subproblems are too complex to have the best performance of the decomposition (since their time horizon is close to the one of the initial problem) and if it is too high, the subproblems are easy to solve but the computing time necessary to solve this high number of subproblems exceeds the one to solve the initial problem. For a time horizon of 20 years, the temporal decomposition is up to 5.6 times faster than the compact resolution.

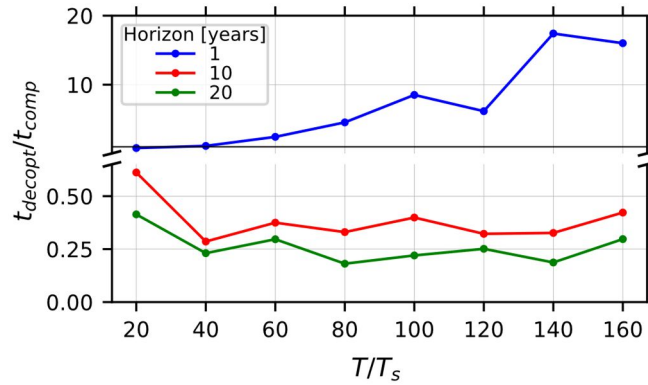


Figure 6: Influence of the time horizon on the computing time
Note: the horizontal line corresponds to $t_{decomp}/t_{comp} = 1$

3.2.4 Influence of the number of CPUs

In this Section, we aim at quantifying the impact of the number of CPUs on the performance of the temporal decomposition. We study the influence of the number of CPUs for the intermediate time horizon (10 years). In Figure 7, we plot the computing times ratio as a function of the ratio T/T_s for several number of CPUs: 16, 24, 32 and 40. A first result is that with an adequate choice of decomposition period, the temporal decomposition is more efficient than the compact resolution for the four numbers of CPUs considered. Moreover, the decomposition period that maximizes the performance of the temporal decomposition depends on the number of CPUs, as the best decomposition period is the one that ensures the most equal repartition of the subproblems amongst the CPUs. For instance, for 32 CPUs, $T/T_s = 60$ is a good choice of decomposition period (as it corresponds to ~ 2 subproblems per CPU) whereas it worsens the performance for 40 CPUs. When the number of CPUs increases from 16 to 40, the temporal decomposition goes from being 1.4 times faster to being 3.5 times faster, i.e. the performance is improved by a factor 2.6 (considering the best decomposition period for each number of CPUs).

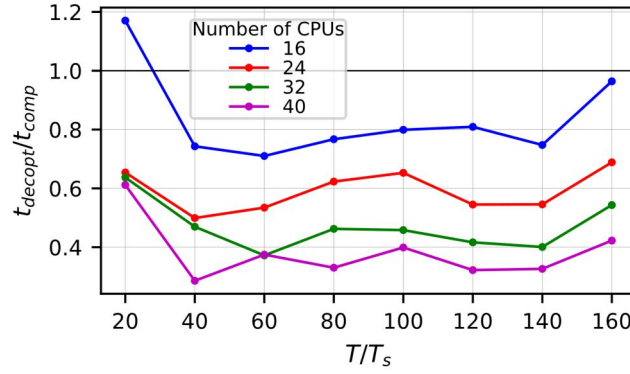


Figure 7: Influence of the number of CPUs on the computing time for a time horizon of 10 years

Note: the horizontal line corresponds to $t_{decept}/t_{comp} = 1$

4 Limitations, future work and implications

Duality properties of MILP, contrary to those of convex problems, are usually not strong, which means that the value of the objective function of the primal problem is not equal to the one of the dual problem [67][68]. Therefore, the dual variables for MILP are not well defined. When the temporal decomposition, described in this work, is used to solve MILP, it needs to retrieve dual variables of MILP. Thus, in some cases, one might encounter convergence difficulties using Benders' algorithm. Moreover, as highlighted in Section 3.2.2, the proposed methodology might not be efficient when the problem is not complex enough (e.g. linear problems). In future works, the proposed methodology could be applied to other case studies (e.g. microgrids connecting numerous dwellings and/or using more detailed models for the PV panels and the batteries).

Despite its limitations, our proposed methodology has the potential to lower computing times. Thus, it could promote the deployment of microgrids, since it makes it possible to account for the whole life cycle to size components in a reduced computing time. Therefore, our work could be useful to microgrids project holders. Moreover, for a future implementation of the decomposition, we have highlighted influential parameters (e.g. the decomposition period).

Conclusion

In this article, we propose a methodology to apply a temporal decomposition based on Benders' algorithm on mixed-integer linear problems to find the optimal planning of microgrids. First, the mathematical formulation for Benders' algorithm, the models used to describe the different components of the microgrid and the optimization problem are introduced. Then, we detail the temporal decomposition which aims at dividing the initial optimization problem into several subproblems with a smaller time interval. Parallelization is used to decrease the computing times of the temporal decomposition. The methodology is applied to a case study and we investigate the influence of different parameters on the performance of the temporal decomposition in terms of computing time: the decomposition period, the nature of the problem, the time horizon and the number of CPUs. First, we highlight the existence of a decomposition period that maximizes the performance of the temporal decomposition: it is a compromise between the number of subproblems and their complexity. Then, we find that the temporal decomposition is more efficient when the problem is a mixed-integer linear problem than when it is a linear problem. Regarding the time horizon, the best performance of the temporal decomposition compared to the compact resolution (resolution without decomposition) is obtained for a time horizon of 20 years using 40 CPUs. With the adequate decomposition period, the temporal decomposition is 5.6 times faster than the compact resolution. Increasing the number of CPUs from 16 to 40 improves the performance of the temporal decomposition by a factor 2.6. The optimal decomposition period depends on the number of CPUs since it guarantees the most even distribution of the subproblems amongst the CPUs. Even though the methodology has been applied to a specific case study, it is generic and transferable to other microgrid optimization problems. Our proposed methodology and results can be useful to researchers and microgrid project holders who aim at finding the optimal sizing and operation of their microgrid within reduced computing times.

CRedit authorship contribution statement

Célia Masternak: Conceptualization, Methodology, Software, Validation, Formal analysis, Investigation, Resources, Writing – Original Draft, Writing – Review & Editing, Visualization, Project administration

Simon Meunier: Conceptualization, Methodology, Validation, Formal analysis, Investigation, Resources, Writing – Review & Editing, Supervision, Project administration

Stéphane Brisset: Conceptualization, Methodology, Resources, Writing – Review & Editing, Supervision, Funding acquisition

Vincent Reinbold: Conceptualization, Methodology, Software, Validation, Formal analysis, Resources, Writing – Review & Editing, Supervision, Project administration, Funding acquisition

Declaration of Competing Interest

The authors declare that they have no known competing financial interests or personal relationships that could have appeared to influence the work reported in this paper.

Acknowledgments

The authors thank Olivier Hubert for his valuable help.

This work was performed using high performance computing resources from the “Mésocentre” computing center of CentraleSupélec and École Normale Supérieure Paris-Saclay supported by CNRS and Région Île-de-France (<http://mesocentre.centralesupelec.fr/>).

This project has received funding from the GDR SEEDS, a research consortium from the French National Centre for Scientific Research (CNRS).

References

- [1] European Commission, “REPowerEU Plan, EU external energy management in a changing world”, May 2022, URL: <https://eur-lex.europa.eu/legal-content/EN/TXT/?uri=JOIN%3A2022%3A23%3AFIN&qid=1653033264976> [Accessed: 05-Jan-23].
- [2] S. Meunier, C. Protopapadaki, R. Baetens, and D. Saelens, “Impact of residential low-carbon technologies on low-voltage grid reinforcements”, *Appl. Energy*, vol. 297: 117057, Sep. 2021, doi: 10.1016/j.apenergy.2021.117057.
- [3] F. Gonzalez, S. Meunier, C. Protopapadaki, Y. Perez, D. Saelens, and M. Petit, “Impact of distributed energy resources and electric vehicle smart charging on low voltage grid stability”, presented at the 26th International Conference and Exhibition on Electricity Distribution (CIRED 2021), p. 1-6, Sept. 2021, doi: 10.1049/icp.2021.2076.
- [4] N. Zaree, V. Vahidinasab, and A. Estebarsari, “Energy Management Strategy of Microgrids Based on Benders Decomposition Method”, presented at the 2018 IEEE International Conference on Environment and Electrical Engineering and 2018 IEEE Industrial and Commercial Power Systems Europe (EEEIC / I&CPS Europe), Palermo, Jun. 2018, pp. 1–6. doi: 10.1109/EEEIC.2018.8494507.
- [5] Y. E. García Vera, R. Dufo-López, and J. L. Bernal-Agustín, “Energy Management in Microgrids with Renewable Energy Sources: A Literature Review”, *Appl. Sci.*, vol. 9, no. 18: 3854, Sep. 2019, doi: 10.3390/app9183854.
- [6] C. Wang, Y. Liu, X. Li, L. Guo, L. Qiao, and H. Lu, “Energy management system for stand-alone diesel-wind-biomass microgrid with energy storage system”, *Energy*, vol. 97, pp. 90–104, Feb. 2016, doi: 10.1016/j.energy.2015.12.099.
- [7] H. Karimi and S. Jadid, “Two-stage economic, reliability, and environmental scheduling of multi-microgrid systems and fair cost allocation,” *Sustain. Energy Grids Netw.*, vol. 28: 100546, Dec. 2021, doi: 10.1016/j.segan.2021.100546.
- [8] X. Liu and B. Su, “Microgrids - an integration of renewable energy technologies,” presented at the 2008 China International Conference on Electricity Distribution (CICED 2008), Guangzhou, China, Dec. 2008, pp. 1–7. doi: 10.1109/CICED.2008.5211651.
- [9] A. Maulik, “Probabilistic power management of a grid-connected microgrid considering electric vehicles, demand response, smart transformers, and soft open points,” *Sustain. Energy Grids Netw.*, vol. 30, p. 100636, Jun. 2022, doi: 10.1016/j.segan.2022.100636.
- [10] E. Dall’Anese, H. Zhu, and G. B. Giannakis, “Distributed Optimal Power Flow for Smart Microgrids”, *IEEE Trans. Smart Grid*, vol. 4, no. 3, pp. 1464–1475, Sep. 2013, doi: 10.1109/TSG.2013.2248175.
- [11] R. Jamalzadeh and M. Hong, “Microgrid Optimal Power Flow Using the Generalized Benders Decomposition Approach”, *IEEE Trans. Sustain. Energy*, vol. 10, no. 4, pp. 2050–2064, Oct. 2019, doi: 10.1109/TSTE.2018.2877907.
- [12] Y. Wang, C. Chen, J. Wang, and R. Baldick, “Research on Resilience of Power Systems Under Natural Disasters—A Review”, *IEEE Trans. Power Syst.*, vol. 31, no. 2, pp. 1604–1613, Mar. 2016, doi: 10.1109/TPWRS.2015.2429656.
- [13] United Nations, Sustainable Development Goals, URL: <https://sdgs.un.org/goals>, [Accessed: 27-Jan-23].
- [14] D. P. e Silva, J. L. Félix Salles, J. F. Fardin, and M. M. Rocha Pereira, “Management of an island and grid-connected microgrid using hybrid economic model predictive control with weather data”, *Appl. Energy*, vol. 278: 115581, Nov. 2020, doi: 10.1016/j.apenergy.2020.115581.
- [15] M. B. Sanjareh, M. H. Nazari, G. B. Gharehpetian, R. Ahmadihangar, and A. Rosin, “Optimal scheduling of HVACs in islanded residential microgrids to reduce BESS size considering effect of discharge duration on voltage and capacity of battery cells,” *Sustain. Energy Grids Netw.*, vol. 25: 100424, Mar. 2021, doi: 10.1016/j.segan.2020.100424.
- [16] M. A. Beyazit, A. Taşçikaraoğlu, and J. P. S. Catalão, “Cost optimization of a microgrid considering vehicle-to-grid technology and demand response,” *Sustain. Energy Grids Netw.*, vol. 32: 100924, Dec. 2022, doi: 10.1016/j.segan.2022.100924.
- [17] B. Li, R. Roche, D. Paire, and A. Miraoui, “Sizing of a stand-alone microgrid considering electric power, cooling/heating, hydrogen loads and hydrogen storage degradation”, *Appl. Energy*, vol. 205, pp. 1244–1259, Nov. 2017, doi: 10.1016/j.apenergy.2017.08.142.
- [18] B. Li, R. Roche, and A. Miraoui, “Microgrid sizing with combined evolutionary algorithm and MILP unit commitment”, *Appl. Energy*, vol. 188, pp. 547–562, Feb. 2017, doi: 10.1016/j.apenergy.2016.12.038.
- [19] N. Dougier, P. Garambois, J. Gomand, and L. Roucoules, “Multi-objective non-weighted optimization to explore new efficient design of electrical microgrids”, *Appl. Energy*, vol. 304: 117758, Dec. 2021, doi: 10.1016/j.apenergy.2021.117758.
- [20] M. F. Zia, E. Elbouchikhi, and M. Benbouzid, “Microgrids energy management systems: A critical review on methods, solutions, and prospects”, *Appl. Energy*, vol. 222, pp. 1033–1055, Jul. 2018, doi: 10.1016/j.apenergy.2018.04.103.
- [21] D. R. Prathapaneni and K. P. Detroja, “An integrated framework for optimal planning and operation schedule of microgrid under uncertainty,” *Sustain. Energy Grids Netw.*, vol. 19: 100232, Sep. 2019, doi: 10.1016/j.segan.2019.100232.
- [22] T. Schütz, X. Hu, M. Fuchs, and D. Müller, “Optimal design of decentralized energy conversion systems for smart microgrids using decomposition methods”, *Energy*, vol. 156, pp. 250–263, Aug. 2018, doi: 10.1016/j.energy.2018.05.050
- [23] S. Boyd, L. Xiao, A. Mutapcic, and J. Mattingley, “Notes on Decomposition Methods,” May 2015, URL: https://web.stanford.edu/class/ee364b/lectures/decomposition_notes.pdf, [Accessed: 10-Feb-23].
- [24] R. Rahmaniani, T. G. Crainic, M. Gendreau, and W. Rei, “The Benders decomposition algorithm: A literature review”, *Eur. J. Oper. Res.*, vol. 259, no. 3, pp. 801–817, Jun. 2017, doi: 10.1016/j.ejor.2016.12.005.
- [25] M. S. Bazaraa, J. J. Jarvis, and H. D. Sherali, *Linear programming and network flows*, 4th ed, Wiley, 2010.
- [26] Y. Liu, H. Beng Gooi, and H. Xin, “Distributed energy management for the multi-microgrid system based on ADMM”, presented at the 2017 IEEE Power & Energy Society General Meeting, Chicago, USA, Jul. 2017, pp. 1–5. doi: 10.1109/PESGM.2017.8274099.
- [27] S. Boyd, “Distributed Optimization and Statistical Learning via the Alternating Direction Method of Multipliers,” *Found. Trends Mach. Learn.*, vol. 3, no. 1, pp. 1–122, 2010, doi: 10.1561/22000000016.
- [28] F. Louveaux and J. R. Birge, L-Shaped Method for Two-Stage Stochastic Programs with Recourse. In: C.A. Floudas, P.M. Pardalos (eds) *Encyclopedia of Optimization*, Boston, MA: Springer US, 2009. doi: 10.1007/978-0-387-74759-0_351.
- [29] R. Kizito, Z. Liu, X. Li, and K. Sun, “Stochastic optimization of distributed generator location and sizing in an islanded utility microgrid during a large-scale grid disturbance,” *Sustain. Energy Grids Netw.*, vol. 27, p. 100516, Sep. 2021, doi: 10.1016/j.segan.2021.100516.

- [30] S. Candas, K. Zhang, and T. Hamacher, “A Comparative Study of Benders Decomposition and ADMM for Decentralized Optimal Power Flow”, presented at the 2020 IEEE Power & Energy Society Innovative Smart Grid Technologies Conference (ISGT), Washington, DC, USA, Feb. 2020, pp. 1–5. doi: 10.1109/ISGT45199.2020.9087777.
- [31] J.F. Benders, “Partitioning procedures for solving mixed-variables programming problems”, *Numer. Math.*, vol. 4, pp. 238–252, Dec. 1962, doi: 10.1007/BF01386316
- [32] A.M. Geoffrion, “Generalized Benders decomposition”, *J Optim Theory Appl*, vol. 10, pp. 237–260, Oct. 1972, doi: 10.1007/BF00934810.
- [33] A. Ibrahim, O. A. Dobre, T. M. N. Ngatched, and A. G. Armada, “Bender’s Decomposition for Optimization Design Problems in Communication Networks”, *IEEE Netw.*, vol. 34, no. 3, pp. 232–239, May 2020, doi: 10.1109/MNET.001.1900414.
- [34] R. Rahmaniani, S. Ahmed, T. G. Crainic, M. Gendreau, and W. Rei, “The Benders Dual Decomposition Method”, *Oper. Res.*, vol. 68, no. 3, pp. 878–895, May 2020, doi: 10.1287/opre.2019.1892.
- [35] Y. Yang, W. Pei, Q. Huo, J. Sun, and F. Xu, “Coordinated planning method of multiple micro-grids and distribution network with flexible interconnection”, *Appl. Energy*, vol. 228, pp. 2361–2374, Oct. 2018, doi: 10.1016/j.apenergy.2018.07.047.
- [36] A. Nagarajan and R. Ayyanar, “Design and scheduling of microgrids using benders decomposition,” presented at IEEE 43rd Photovoltaic Specialists Conference (PVSC), Portland, USA, Jun. 2016, pp. 1843–1847. doi: 10.1109/PVSC.2016.7749940.
- [37] J. Wei, Y. Zhang, J. Wang, X. Cao, and M. A. Khan, “Multi-period planning of multi-energy microgrid with multi-type uncertainties using chance constrained information gap decision method”, *Appl. Energy*, vol. 260: 114188, Feb. 2020, doi: 10.1016/j.apenergy.2019.114188.
- [38] A. Khodaei, “Microgrid Optimal Scheduling With Multi-Period Islanding Constraints,” *IEEE Trans. Power Syst.*, vol. 29, no. 3, pp. 1383–1392, May 2014, doi: 10.1109/TPWRS.2013.2290006.
- [39] M. A. Abdulgalil, M. Khalid, and F. Alismail, “Optimizing a Distributed Wind-Storage System Under Critical Uncertainties Using Benders Decomposition,” *IEEE Access*, vol. 7, pp 77951–77963, 2019, doi: 10.1109/ACCESS.2019.2922619.
- [40] Z. K. Pecenek, M. Stadler, and K. Fahy, “Efficient multi-year economic energy planning in microgrids”, *Appl. Energy*, vol. 255: 113771, Dec. 2019, doi: 10.1016/j.apenergy.2019.113771.
- [41] B. Mukhopadhyay and D. Das, “Optimal multi-objective long-term sizing of distributed energy resources and hourly power scheduling in a grid-tied microgrid,” *Sustain. Energy Grids Netw.*, vol. 30: 100632, Jun. 2022, doi: 10.1016/j.segan.2022.100632.
- [42] S. Hemmati, S. F. Ghaderi, and M. S. Ghazizadeh, “Sustainable energy hub design under uncertainty using Benders decomposition method”, *Energy*, vol. 143, pp. 1029–1047, Jan. 2018, doi: 10.1016/j.energy.2017.11.052.
- [43] S. Montoya-Bueno, J. Muñoz-Hernandez, J. Contreras, and L. Baringo, “A Benders’ Decomposition Approach for Renewable Generation Investment in Distribution Systems”, *Energies*, vol. 13, no. 5: 1225, Mar. 2020, doi: 10.3390/en13051225.
- [44] T. H. Kim, H. Shin, K. Kwag, and W. Kim, “A parallel multi-period optimal scheduling algorithm in microgrids with energy storage systems using decomposed inter-temporal constraints”, *Energy*, vol. 202: 117669, Jul. 2020, doi: 10.1016/j.energy.2020.117669.
- [45] H. Xiong, Z. Chen, Y. Zhang, C. Wang, and C. Guo, “Robust Dispatch with Temporal Decomposition of Integrated Electrical-Heating System Considering Dynamic Reserve Domain”, presented at the 2021 IEEE 2nd China International Youth Conference on Electrical Engineering (CIYCEE), Chengdu, China, pp. 1–7, Dec. 2021, doi: 10.1109/CIYCEE53554.2021.9676746.
- [46] S. Brisset and M. Ogier, “Collaborative and multilevel optimizations of a hybrid railway power substation”, *Int. J. Numer. Model. Electron. Netw. Devices Fields*, vol. 32, no. 4, Jul. 2019, doi: 10.1002/jnm.2289.
- [47] V. Reinbold, V.-B. Dinh, D. Tenfen, B. Delinchant and D. Saelens, "Optimal operation of building microgrids – comparison with mixed-integer linear and continuous non-linear programming approaches", *COMPEL*, Vol. 37 No. 2, pp. 603-616, Mar. 2018, doi: 10.1108/COMPEL-11-2016-0489
- [48] A. McEvoy, T. Markvart, and L. Castañer, *Practical Handbook of Photovoltaics - Fundamental and Applications*, 2nd ed, Academic Press, 2011.
- [49] C. Soenen, V. Reinbold, S. Meunier, J.A. Cherni; A. Darga, P. Dessante, L. Quéval, “Comparison of Tank and Battery Storages for Photovoltaic Water Pumping”, *Energies*, vol. 14, no. 9: 2483, Apr. 2021, doi: 10.3390/en14092483.
- [50] L. A. Wolsey, “Integer programming duality: Price functions and sensitivity analysis,” *Math. Program.*, vol. 20, no. 1, pp. 173–195, Dec. 1981, doi: 10.1007/BF01589344.
- [51] M. L. Bynum, G.A. Hackebeil, W. E. Hart, C. D. Laird, B. L. Nicholson, J. D. Sirola, J-P. Watson, D. L. Woodruff, “Pyomo — Optimization Modeling in Python”, vol. 67. Cham: Springer International Publishing, 2021. doi: 10.1007/978-3-030-68928-5.
- [52] V. Reinbold, “LMS2 Library”, URL: https://reinboldv.github.io/lms2/docs/_build/html/index.html, [Accessed: 13-Feb-23].
- [53] Mésocentre du Moulon, URL: <http://mesocentre.centralesupelec.fr/>, [Accessed: 09-Jan-23].
- [54] R. Dufo-López, J. L. Bernal-Agustín, and J. Contreras, “Optimization of control strategies for stand-alone renewable energy systems with hydrogen storage”, *Renew. Energy*, vol. 32, no. 7, pp. 1102–1126, Jun. 2007, doi: 10.1016/j.renene.2006.04.013.
- [55] D. Tenfen and E. C. Finardi, “A mixed integer linear programming model for the energy management problem of microgrids”, *Electr. Power Syst. Res.*, vol. 122, pp. 19–28, May 2015, doi: 10.1016/j.epsr.2014.12.019.
- [56] Sunrun Team, “What Is the Life Expectancy of a Solar Battery?”, Mar. 2019, URL: <https://www.sunrun.com/go-solar-center/solar-articles/what-is-the-life-expectancy-of-a-solar-battery#:~:text=How%20Long%20Does%20a%20Solar,of%20your%20solar%20power%20system>, [Accessed: 16-Dec-22].
- [57] Meritsun, “Power House Lithium ion Battery”, URL: <https://www.meritsunpower.com/10-years-warranty-6000-cycle-life-5kwh-power-house-lithium-ion-battery-48v-100ah-solar-battery-with-lcd-display>, [Accessed: 16-Dec-22].
- [58] “EEG 2023: Das ändert sich für Photovoltaik-Anlagen“, Oct. 2022 URL:<https://www.verbraucherzentrale.de/wissen/energie/erneuerbare-energien/eeg-2023-das-aendert-sich-fuer-photovoltaikanlagen-75401>, [Accessed: 15-10-22].

- [59] L. De Boeck, S. Van Asch, P. De Bruecker, and A. Audenaert, “Comparison of support policies for residential photovoltaic systems in the major EU markets through investment profitability”, *Renew. Energy*, vol. 87, pp. 42–53, Mar. 2016, doi: 10.1016/j.renene.2015.09.063.
- [60] A. Gong, “Understanding PV system losses”, *Aurora Sol*, 2018, URL: <https://www.aurorasolar.com/blog/understanding-pv-system-losses-part-1/>, [Accessed: 25-Jan-23].
- [61] A. Yıldız, T. Gökçek, İ. Şengör, and O. Erdinç, “Optimal sizing and economic analysis of Photovoltaic distributed generation with Battery Energy Storage System considering peer-to-peer energy trading”, *Sustain. Energy Grids Netw.*, vol. 28: 100540, Dec. 2021, doi: 10.1016/j.segan.2021.100540.
- [62] S. Meunier, L. Quéval, A. Darga, P. Dessante, C. Marchand, M. Heinrich, J. A. Cherni, E. A. de la Fresnaye, L. Vido, B. Multon, “Sensitivity Analysis of Photovoltaic Pumping Systems for Domestic Water Supply”, *IEEE Trans. Ind. Appl.*, vol. 56, no. 6, pp. 6734–6743, Nov. 2020, doi: 10.1109/TIA.2020.3013513.
- [63] J. Heidjann, “Aktuelle Strompreise für Haushalte“, 2022, URL: <https://www.stromauskunft.de/strompreise/>, [Accessed: 21-Nov-22].
- [64] European Commission, “Copernicus Atmosphere Monitoring Service (CAMS)”, Nov. 2014, URL: <http://www.soda-pro.com/web-services/radiation/cams-radiation-service>, [Accessed: 03-Feb-23].
- [65] M. Schlemminger, T. Ohrdes, E. Schneider, and M. Knoop, “Dataset on electrical single-family house and heat pump load profiles in Germany,” *Sci. Data*, vol. 9, no. 1, p. 56, Dec. 2022, doi: 10.1038/s41597-022-01156-1.
- [66] S. A. Alves dos Santos, J. P. N. Torres, C. A. F. Fernandes, and R. A. Marques Lameirinhas, “The impact of aging of solar cells on the performance of photovoltaic panels,” *Energy Convers. Manag. X*, vol. 10: 100082, Jun. 2021, doi: 10.1016/j.ecmx.2021.100082.
- [67] H. P. Williams, “Duality in mathematics and linear and integer programming”, *Journal of Optimization Theory and Applications*, vol. 90, pp. 257-278, Aug. 1996, doi: 10.1007/BF02189998.
- [68] M. Guzlsoy, and T.K. Ralphs, “Duality for mixed-integer linear programs”, *Internat. J. Oper. Res.*, vol. 4, no. 3, pp. 118-137, 2007.